Dynamic electrochemistry with ionophore based ion-selective membranes

Crespo Paravano, Gaston Adrian; Bakker, Eric

RSC Advances

RSC Publishing

REVIEW

Dynamic electrochemistry with ionophore based ion-selective membranes

Cite this: *RSC Adv.*, 2013, **3**, 25461

Gastón A. Crespo and Eric Bakker*

This review outlines key principles and recent advances in the use of dynamic electrochemistry with polymeric liquid membranes. Ideally polarizable membranes are most attractive in fundamental studies of ion transfer and when the accumulation of the ion in the receiving phase is of key interest, for example in stripping ion transfer voltammetry. All solid-state membranes doped with conducting polymers have exhibited attractive low detection limit for hydrophilic ions. On the other hand, initially non-polarized interfaces are most useful when one aims to effect a concentration change of an ionic species in the sample phase. Conveniently, these types of membranes can be interrogated with potentiometry and sequentially with dynamic techniques such as chronopotentiometry. This can be used to obtain speciation information as they allow one, in principle, to assess total labile and free ion concentrations in the same experiment. A number of electrochemical techniques have been reported and include controlled potential techniques such as cyclic voltammetry, normal pulse voltammetry, stripping voltammetry and thin layer coulometry as well as current controlled ones such as pulsed chronopotentiometry and flash chronopotentiometry. All of these techniques have their purpose and strength.

Received 19th July 2013
Accepted 4th October 2013

DOI: 10.1039/c3ra43751e

www.rsc.org/advances

1. Introduction

Polymeric liquid membranes are well established as a robust analytical materials platform for developing electrochemical ion sensors that have become important tools in clinical diagnostics and environmental monitoring for the detection of a wide range of ionic species. Fundamentally, they work on the basis of ion partitioning and host–guest chemical principles. A wide variety of chemical host molecules (ionophores) have been developed that induce a selectivity pattern that deviates from the one imposed by the so-called Hofmeister selectivity sequence.

Department of Inorganic and Analytical Chemistry, University of Geneva, Quai Ernest-Ansermet 30, CH-1211 Geneva, Switzerland. E-mail: eric.bakker@unige.ch; Tel: +41 22 379 6431

Gastón A. Crespo is currently a postdoctoral researcher at the University of Geneva, where he has been since early 2011. After his childhood and a university education in Buenos Aires (Argentina) he pursued his Ph.D. studies in Tarragona, Spain (2010), before moving to his current position. His research focuses on new electrochemical sensing concepts based on membrane electrodes. He has co-authored more than 30 publications so far.

Eric Bakker is Professor of Analytical Chemistry at the University of Geneva since 2010. He received his Ph.D. at ETH Zurich in Switzerland in 1993, after which time he pursued postdoctoral studies at the University of Michigan in Ann Arbor, U.S.A. His first faculty position was at Auburn University (U.S.A.) where he rose to the rank of full professor. He moved to his current position after appointments at Purdue University, U.S.A., and Curtin University in Perth, Western Australia. Eric Bakker's research interests are in the application of extraction, complexation and ion transport principles to Analytical Chemistry, with a special emphasis on the development of chemical sensors. He has co-authored ca. 220 publications so far that have been globally cited over 11 000 times.

While most polymeric membranes are chiefly operated by potentiometry, a number of attractive analytical features have recently been reported when such membranes are interrogated by either controlled current or potential techniques. Examples for such advances include stripping ion transfer voltammetry, where low detection limits due to analyte accumulation is combined with diagnostic power as the stripping potential gives information about the nature of the ion. Pulsed techniques have allowed one to switch ion selectivity and even the charge type of the detected ion in a single experiment. Much higher sensitivities relative to that normally observed with ion-selective electrodes have been observed. Chemical species that ordinarily poison a membrane can be discriminated against kinetically and hence tolerated. Polyionic species such as heparin or protamine can now be measured reversibly, while they poison their potentiometric counterparts. Adequately designed membrane electrodes can be used for speciation analysis in tandem with zero current potentiometry. Finally, thin layer ion transfer voltammetry is an attractive platform to design potentially calibration free ion sensors.

These exciting recent advances were made possible by bringing two previously separate fields together, electrochemistry at the interface of two immiscible electrolyte solutions (ITIES), formed and dominated by physical electrochemists, and ion-selective electrodes (ISEs), the historical domain of analytical chemists. This review first approaches the field of dynamic electrochemistry at ion-selective electrodes from the perspective of ITIES, with an introduction of ideally polarizable membranes. We then move to systems closer to ion-selective electrodes by the use of permselective membranes that can be coined initially non-polarized membranes. A brief introduction into the working principles precedes a discussion of recent advances for each direction.

2. Ideally polarizable membranes

Membranes that do not exhibit ion-exchanger properties are called ideally polarizable membranes. In the absence of an ion-exchanger, the phase boundary potential at the sample–membrane interface, in the absence of current, is not clearly defined and potentiometric readout is inadequate. However, a range of dynamic electrochemistry techniques can be used in order to establish successful ion transfer voltammetric readout.

2.1 Working principles for ideally polarizable membranes

The ion-transfer voltammetry at the interface of two immiscible electrolyte solutions (ITIES) forms the fundamental basis for this first class of techniques.[1–6] The potential provides the required energy to polarize the interface and to subsequently transfer ions from one phase to the other, giving rise to a faradaic current. This process bears some analogy to that at metal–solution interfaces in the presence of an electro-active species but does not require an oxidation–reduction reaction of the transferred analyte.

A number of solvent systems were explored at the ITIES, but the interface formed by water and nitrobenzene is most widely established. Here, hydrophilic (I^+A^-, aqueous phase) and lipophilic (R^+R^-, organic phase) electrolytes are added to and ideally confined within each respective phase in the absence of electrochemical stimulation. A potential sweep between two reference elements placed in the bulk of each individual phase may result in a observable ion transfer from the aqueous to the organic phase, typically detected as a current at two counter electrodes, thereby requiring a four-electrode potentiostat.

Fig. 1a illustrates the ion-transfer process between phase α (aqueous phase) and β (organic phase). Within the potential window, capacitive charging is observed as a relatively small and relatively constant current. Around the ion transfer potential, a faradaic current is observed that originates from the requirement to fulfill eqn (1) (see Fig. 1b).

$$E_{PB} = \Delta_{\alpha}^{\beta}\phi_j^0 - \frac{RT}{z_j F}\ln\frac{a_j^{\beta}(0)}{a_j^{\alpha}(0)} \quad (1)$$

where $\Delta_{\alpha}^{\beta}\phi_j^0$ is the standard transfer potential, which is a function of the free energies of transfer of the ion and hence of the solvation energies in either phase, a_j is the activity of the ion j with charge z_j in the indicated phase α (typically aqueous) or β (typically organic), at the phase boundary (position 0 as indicated). A cathodic applied potential may either result in the extraction of a cation (I^+) from phase α to β or an anion (R^-) from phase β to α. Conversely, an anodic applied potential may promote the extraction of an anion (A^-) from phase α or a cation (R^+) from phase β. The ion transfer process is visualized by a current response. As eqn (1) is valid for the interface, any transferred ion is continually lost by mass transport into the bulk of the receiving phase and needs to be replenished. The observed current is directly proportional to the net ion flux.

Electrochemical ion transfer is generally described as a function of both free energy and ion activity, see eqn (1). Evidently, the transfer of one ion over the other will be favored if it exhibits a lower free energy of transfer. The presence of a selective complexing agent (so-called ionophore) in the receiving phase results in a milder required potential to achieve the ion transfer (Fig. 1c). In this case, one also speaks of assisted ion transfer.

The experimental setup may be simplified in order to avoid the use of lipophilic reference electrodes and bulky solutions by sandwiching the organic phase between two aqueous phases to form a membrane. As a consequence, we are now counting two interfaces (α-outer and α′-inner). Depending on the selected electrolyte either one or both interfaces can be polarized.

The electrochemical cell shown in eqn (2) consists a single polarized interface (α|β):

$$RE|I^+A^-(\alpha)|R^+R^-(\beta)|R^+B^-(\alpha')|RE \quad (2)$$

The interface β|α′ is a non-polarizable interface because the ion R_1^+ is shared between both phases. Consequently, the potential at this second interface is considered to be constant in the course of the experiment. Unfortunately, this configuration may fail if ionophores are incorporated in the phase β aiming to facilitate ion transport because of spontaneous ion-exchange of R^+ with the ion of interest.

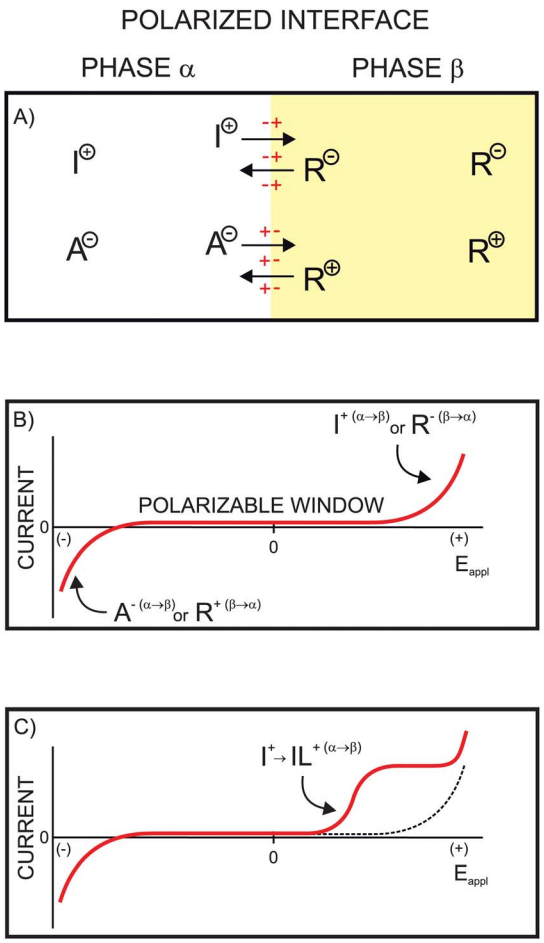

Fig. 1 Ideally polarized interfaces. (a) The interface is composed of two immiscible phases (α and β). Each one contains either hydrophilic (I^+A^-) or lipophilic (R^+R^-) salts. Ion-transfer is established when either cathodic or anodic potential is applied to the electrochemical cell. Cathodic potentials (+) might provoke the ion transfer of I^+ (α → β) or R^- (β → α). Conversely, anodic potentials may establish the ion transfer of A^- (α → β) or R^+ (β → α). (b) Schematic illustration of an expected voltammogram. In the absence of ion transfer, only a capacitive current is recorded (polarizable window). An increase of output current is observed once the ion transfer process takes place. (c) Incorporation of ionophore (L) into the organic phase may facilitate the cation-transfer due to the strong complexation (IL^+, β). As a result, the cation-transfer occurs at milder potentials than in the absence of ionophore (dashed line).

Eqn (3) describes an electrochemical cell with two polarizable interfaces (α|β and β|α′). If the electrolyte R^+R^- is sufficiently lipophilic, the cathodic transfer of the cation I^+ from phase α to β must be accompanied with the transfer of the anion B^- from phase α′ to β at the second interface. Since the lipophilic species does no longer need to be dissolved in the aqueous phase α′, more lipophilic electrolytes R^+R^- may be used for improved robustness compared to the case shown above in eqn (2).

$$RE|I^+A^-(\alpha)|R^+R^-(\beta)|J^+B^-(\alpha')|RE \quad (3)$$

If one assumes that mass transport occurs predominantly by diffusion, a cathodic current will be a function of the concentration gradient, the diffusion layer thickness and diffusion coefficient, in agreement with Fick's first law. For one-dimensional diffusion with the interface at position 0 and the coordinates x for phase β and y for phase α, one may write for the current i:

$$\frac{i}{z_jFA} = D_j^{\beta}\left(\frac{\partial c_j(x)}{\partial x}\right)_{x=0} = -D_j^{\alpha}\left(\frac{\partial c_j(y)}{\partial y}\right)_{y=0} \quad (4)$$

where D_j is the diffusion coefficient of j in the indicated phase and A is the effective interfacial area. Evidently, the current across the interface may be limited by ion diffusion on either side of the interface (see Fig. 2). Note that current is denoted here with a lowercase i in order to avoid confusion with the naming of the primary analyte (I^+) in this text.

2.2 Ion-transfer voltammetry

Electrochemical ion-transfer experiments have typically been performed by cyclic voltammetry. A sweep potential allows one

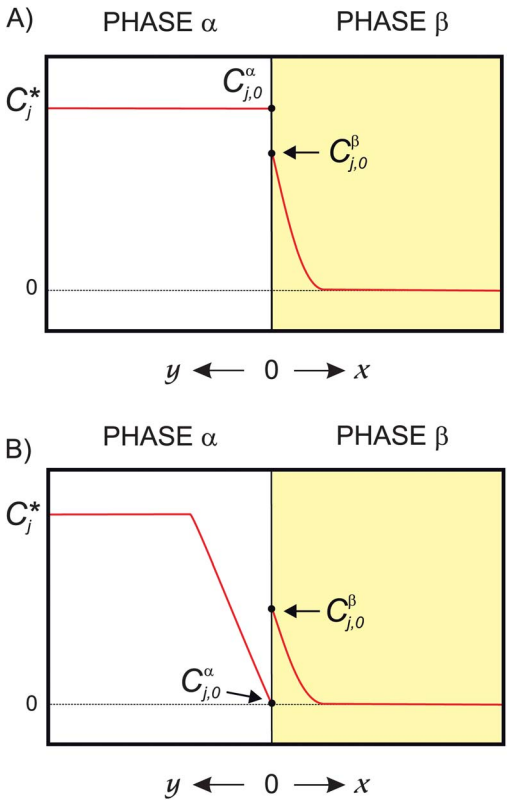

Fig. 2 Illustration of diffusion concentration profiles established at cathodic applied potentials. At the beginning of the experiment, the concentration of j^+ in the receiving phase (β) is near zero and the concentration of j^+ in the sample phase corresponds to the bulk concentration (C_j^*). (a) The current is limited by ion-diffusion in the organic phase. Ion j^+ accumulates at the membrane side of the phase boundary (position 0, $C_{j,0}^{\beta}$). The aqueous phase ion profile is approximately constant during the experiment. This configuration is chiefly used in order to investigate characteristics in the membrane. (b) Current across the interface is limited by ion diffusion in aqueous phase. The ion j^+ depletes in the outer phase boundary (position 0, $C_{j,0}^{\alpha} \sim 0$). Accumulation in the receiving phase is also established with $C_{j,0}^{\beta}$ but is not the limiting process. This approach is more frequently employed for developing ion sensors. x and y are the spatial coordinates for both phases, as indicated.

to obtain useful information about the electrochemical characteristics of the ion transfer process, such as the ion-transfer potential and the reversibility of ion transfer.[7–14]

If only one polarized interface is considered, see eqn (2), the phase boundary potential (E_{pb}) is expressed as a function of the activity of I^+ in both phases (eqn (1)). As stated above, E_{pb} is not clearly defined in the absence of an external potential. Only when the applied E_{pb} approaches the standard potential, the cation has to be transferred to the membrane phase in order to fulfill eqn (1). The equation may be satisfied by either a decrease of a_j^{α} or an increase of a_j^{β}.

In analytical applications, one typically aims to limit the current by diffusion in the aqueous phase, and for this purpose, relatively large diffusion coefficients in the receiving phase β are desirable. Fig. 3 illustrates the general shape and position of an ion-transfer wave relative to the background current when the current is limited by diffusion in the aqueous phase.

Standard ion transfer potentials ($\Delta_{\alpha}^{\beta}\phi_j^0$) were determined for numerous ions by cyclic voltammetry. The ion transfer of hydrophilic ions such as H^+, Li^+, Na^+, K^+, Rb^+, Cs^+, F^-, Cl^-, I^-, NO_3^-, ClO_4^-, SCN^- and lipophilic ions such as quaternary ammonium cations or tetraphenylborate anions were characterized (see the review of Samec for more information).[6]

In order to improve the electrochemical setup, Arrigan and Amemiya have recently moved to micro and nano-liquid interfaces.[10,15–22] Both ohmic drop and capacitive currents are dramatically diminished utilizing these ultra-small liquid–liquid interfaces. For instance, nanopipets, micro and nanofabrication are used to develop massive sensor arrays.

Gelified organic solvents, such as nitrobenzene with a few percent of dissolved PVC, were used to obtain interfaces with improved mechanical stability,[23,24] such systems exhibit *ca.* 10 times smaller diffusion coefficient than in liquids. On the other hand, liquid polymeric membranes used in ion-selective electrodes were first evaluated by cyclic voltammetry in the 80s. The diffusion coefficients in such membranes are about one hundred to one thousand times smaller than in aqueous solutions. At elevated sample concentrations, therefore, one will more easily observe a current that is limited by mass transport in the organic phase. In this case, one may obtain important information about the membrane such a transport and binding properties.

Buck, Pungor and Horvai were the first to explore cyclic voltammetry on polymeric liquid membranes.[25,26] For instance, Horvai *et al.* reported on the reversible ion-transfer of either tetraphenylborate or tetrahexylammonium ions from the membrane to the aqueous phase under polarization conditions of ±0.4 V (the membrane was composed of the salt of these two ions).[27]

Later, the group of Bakker aimed to develop the ion-transfer concept to a useful analytical tool. For this purpose, polymeric membranes doped with a very lipophilic salt (ETH 500) were studied in cyclic voltammetry.[28] Since all components exhibited a very high lipophilicity, the only possible mechanism corresponds to the extraction of the hydrophilic ions at both interfaces (see eqn (3) above, Fig. 4). As a result both sides of the membrane are considered as ideally polarizable interfaces as was previously mentioned, but contrary to previous examples, both hydrophilic cations and anions presented in the sample compartment may be traced in the same scan. This type of experiment was performed with ionophores in the membrane phase as well.[29]

Once the forward sweep scan is applied, the extracted ions will start to accumulate in and diffuse into the membrane

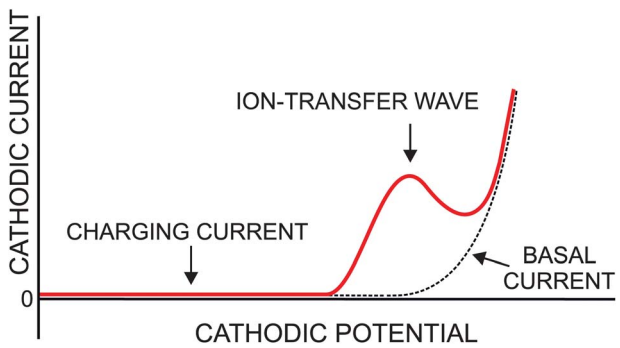

Fig. 3 Schematic illustration of voltammetric ion transfer. Capacitive currents are observed at milder applied potentials. At higher potential amplitudes, the induced ion transfer is visualized with a characteristic current peak. At more extreme cathodic potentials, the background electrolyte starts to be transferred as well. Basal current and ion transfer voltammogram converge at the end of the scan.

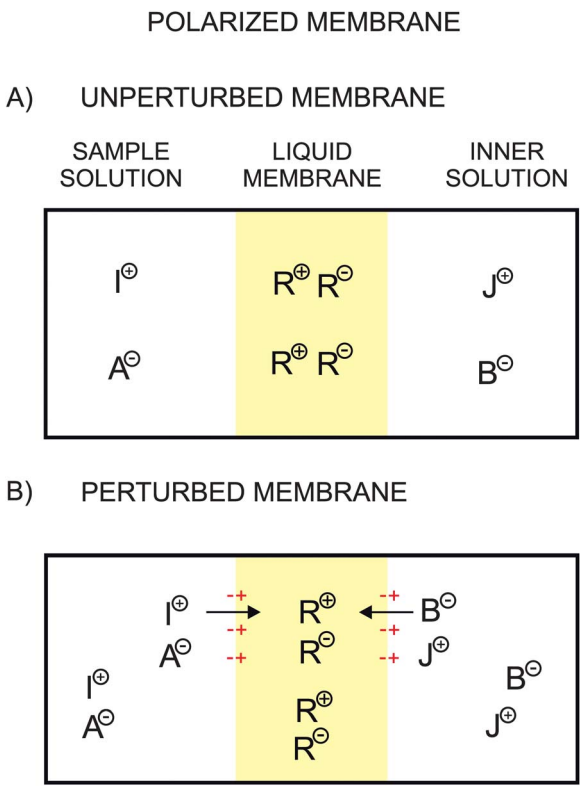

Fig. 4 Illustration of the ion transfer mechanism for membranes containing two ideally polarized interfaces. (a) Unperturbed membrane containing a very lipophilic electrolyte (R^+R^-). Both aqueous phases have hydrophilic components (I^+A^- for the sample solution and B^+J^- for the inner solution). The phase boundary potential is not defined for this unperturbed state. (b) Once a cathodic potential (or current) is applied to the electrochemical cell, I^+ is transferred to the receiving phase. This latter process is coupled to the backside extraction of B^-.

phase. It was shown that a simple backward sweep does not allow for sufficient time to back-extract these ions into their respective aqueous phases. For this reason, cyclic voltammetry is not the most appropriate analytical method for this type of system. Normal pulse voltammetry was introduced to allow for sufficient back-extraction time and an improved signal reproducibility.[30] When the baseline period was chosen as 20-times longer than the extraction pulse, the reproducibility was found to be around 1%. More sophisticated instrumental protocols such as stripping voltammetry, pulsed-chronopotentiometry and flash chronopotentiometry were introduced by this author and other groups to maximize the quality of the analytical sensing parameters.

2.3 Ion-transfer stripping voltammetry

Ion-transfer stripping voltammetry (ITSV) is a well-established analytical technique that allows one to interrogate liquid–liquid interfaces as well as polymeric membranes.[31] In fact, it was chiefly introduced in order to transform ion-transfer voltammetry into a more suitable and useful analytical tool. Specifically, it has the potential to significantly improve the detection limit for dilute ion concentrations that have important environmental and biomedical implications.

Similar to stripping voltammetry on metal electrodes, the analyte ion is potentiostatically transferred from the aqueous phase to the receiving membrane phase (pre-concentration step). Later, an enhanced response is obtained by stripping the pre-concentrated analyte from the membrane to the aqueous phase.

Marecek and Samec explored this technique for hydrophilic ions such as transition and alkaline earth metals (Fig. 5a) with liquid interfaces.[32–37] Afterwards, lipophilic ions such as acetylcholine,[38,39] vitamin B1,[40] amines, surfactants,[41–43] β-blocker propranolol,[15,44] proteins[45] and others were also determined with similar interfaces. Even though this technique displayed attractive performance, the electrochemical setup is perhaps too delicate for routine applications. In analogy to the transition of mercury drop to mercury film electrodes, better recoveries and sharper stripping peaks may be observed with a thin membrane.

Instead of using a hanging organic electrolyte drop, Senda used a gelified organic phase (organic solvent to PVC mass ratio of 2 : 1) in order to achieve a thinner layer of about 50 μm.[46] LiCl was used as background electrolyte in both aqueous phases and a tetraphenylborate derivative served as the common anion in phases α′ and β in order to create a non-polarizable interface at the backside of the membrane. As shown in the following Fig. 5b, stripping ion transfer voltammetry of mercury ions was demonstrated down to the 20 nM concentration range with 10 mM serving as ionophore in the organic phase.

As discussed further below, the group of Amemiya made major contributions to this technique by moving to an all solid-state membrane configuration.

2.4 Pulsed chronopotentiometry

In this technique, a current is applied across the membrane and the resulting cell potential is observed. This gives ion transfer

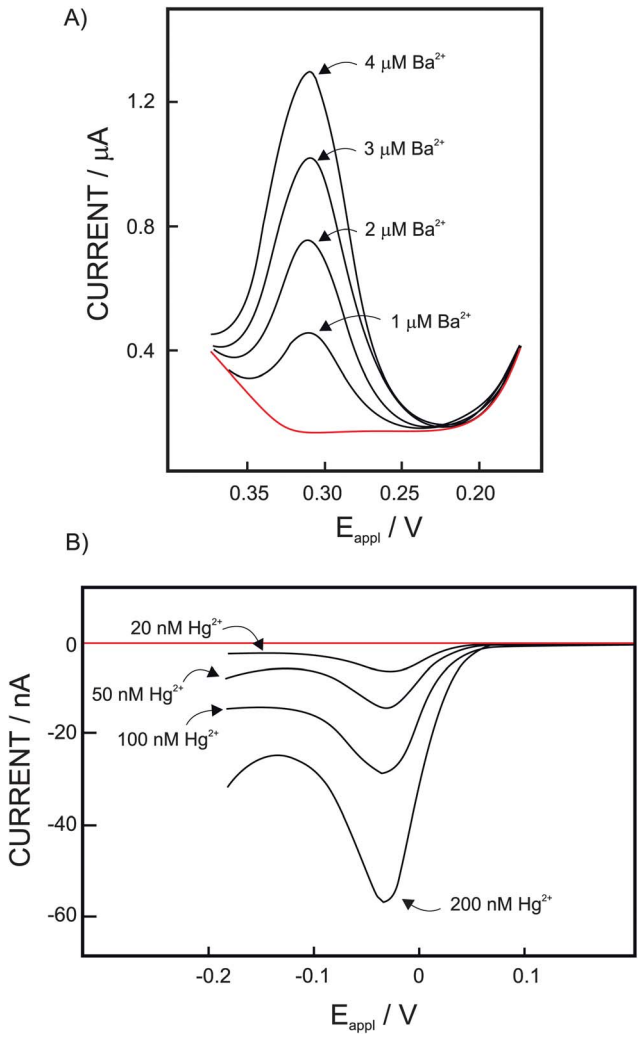

Fig. 5 (a) Stripping ion transfer voltammetric determination of micromolar concentrations of barium at a hanging electrolyte drop electrode.[33] (b) Stripping ion transfer voltammetry at a PVC-based free hanging membrane.[46]

voltammetry responses that bear some analogy to that of potentiometric sensors, with a number of possible advantages. A polymeric membrane without perm-selective properties may be obtained with a lipophilic electrolyte ($R_1^+R_2^-$, both ions are lipophilic) and an appropriate ionophore L (selective for I^+) in the membrane. The cell is otherwise in analogy to that shown in eqn (3) and may be represented in eqn (5) as follows:

$$RE|I^+A^-(\alpha)|R_1^+R_2^-, L(\beta)|J^+B^-(\alpha')|RE \quad (5)$$

As a cathodic current is applied across the membrane, I^+ is transferred from the sample (α) to the membrane phase. Here, the transfer is assisted by the ionophore L, which forms a reversible complex with I^+. As mentioned above, B^- is extracted from the inner solution side (α′) to maintain electroneutrality.

Assuming that diffusion is the dominant mode of transport, different situations can be established (see eqn (4)). At elevated sample concentrations of I^+, one may eventually neglect the

concentration polarization in the aqueous phase. At a given potential sampling time t, and for a selective ion transfer (only I^+ may extract from the sample side), the diffusion layer assumes a defined thickness in the membrane, $\delta(t)$. With a negligible concentration of I^+ in the membrane bulk, a relationship between cathodic current and membrane phase boundary concentration (at position 0) may therefore be expressed:

$$\frac{i}{FA} \approx \frac{D^{\beta}_{IL^+}}{\delta^{\beta}_{IL^+}(t)} c^{\beta}_{IL^+}(0,t) \quad (6)$$

This relationship suggests that the membrane phase boundary concentration of analyte ion can be imposed by the applied current and the potential sampling time.

Consider now the phase boundary potential eqn (1) above by assuming that $c^{\beta}_{IL^+}(0,t)$ is proportional to $a^{\beta}_{j}(0,\ t)$, which is reasonably correct if the membrane contains a large excess of ionophore and the activity coefficient is approximately constant.

We now rewrite the phase boundary potential eqn (1) to obtain a Nernst-like equation:

$$E_{PB} = A(t) + \frac{RT}{F} \ln a^{\alpha}_{I^+} \quad (7)$$

The term $A(t)$ is dependent on the sampling time, t. For an inner solution containing just a single electrolyte at high concentration (no concentration polarization), similar equations may be developed for the inner membrane phase boundary. Since the inner solution composition remains constant in the course of the experiment, the contribution of the inner boundary potential to the overall potential remains indifferent of the sample composition.

The pulsed chronopotentiometry technique can be used in two operative modes that depend on the concentration of the analyte. On the one hand, at high sample concentrations, the amplitude of the applied current and, to a lesser extent, the sampling time, dictates the concentration of ions extracted into the membrane phase boundary. This may be used to modulate membrane selectivity. On the other hand, at lower sample concentrations, the experiment may be used to deplete the analyte at the sample side of the membrane. One may formulate the flux equation for the aqueous ions as follows:

$$\frac{i}{FA} \approx \frac{D^{\alpha}_{I^+}}{\delta^{\alpha}_{I^+}(t)} \left(c^{*}_{I^+} - c^{\alpha}_{I^+}(0,t)\right) \quad (8)$$

where $c^{*}_{I^+}$ indicates the concentration in the sample bulk. For a fixed current and sampling time, t, a bulk concentration exists at which the phase boundary concentration locally depletes. This concentration is the point in the calibration curve where a sharp super-Nernstian potential step occurs. It may be approximated from the Sand equation as follows in (eqn (9)).

$$c^{*}_{I^+}(\text{step}) \approx \frac{2i}{FA}\left(\frac{t}{\pi D^{\alpha}_{I^+}}\right)^{1/2} \quad (9)$$

The location of this step is the point of maximum sensitivity for the membrane electrode. At a chosen critical concentration, very high changes in potential may be observed by subtracting two potentials observed at slightly different applied current values.

The pulsed chronopotentiometry concept was introduced in order to provide a more robust read-out for polymeric membranes. In this way, a short galvanostatic pulse (1–5 s) is used to polarize both interfaces (Fig. 6).[47,48] In contrast to controlled potential techniques, controlled current defines a precise and constant net flux.

Using an appropriate protocol, the membrane is preferentially regenerated under controlled potential conditions. Applying the open circuital potential of the membrane measured before the galvanostatic pulse displays reproducible signals.[49] A sequence of galvanostatic (interrogation) and potentiostatic (regeneration) pulses was established as electrochemical protocol for fundamental studies and applications where such polymeric membranes were involved, and such membrane electrodes are coined *pulstrodes*.

Such pulstrodes exhibit a near-Nernstian response in complete analogy to zero current potentiometry (with membranes containing ion-exchanger properties) when the potential magnitude in the end of the galvanostatic pulse is recorded as a function of the primary analyte activity in the sample. Fig. 7 illustrates the comparison between two different membranes operated under zero current potentiometry (permselective membrane) and pulsed chronopotentiometry (non-permselective membrane). Both methods provide the expected Nernstian responses at high sample concentrations. In addition, the super Nernstian behavior is more significant when the membrane is operated by pulsed chronopotentiometry. The amplitude of the current controls the interfacial concentration of extracted ions and provides a means by which the membrane selectivity can be tuned. Additionally, it was observed that the observed drift at lower concentrations in potentiometry could be eliminated using pulsed chronopotentiometry. In subsequent years, pulsed chronopotentiometry was used to determine, for instance, total calcium[50] and polyions (such as

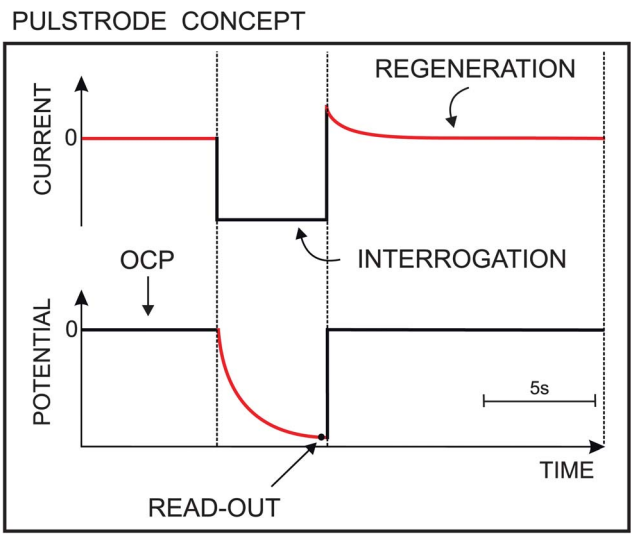

Fig. 6 Pulstrode concept. The membrane is interrogated with a sequence of three pulses. (i) Open circuit potential is determined at zero current; (ii) galvanostatic interrogation pulse (output: potential decay, the last point is considered as signal); (iii) open circuital potential is applied to regenerate the membrane.

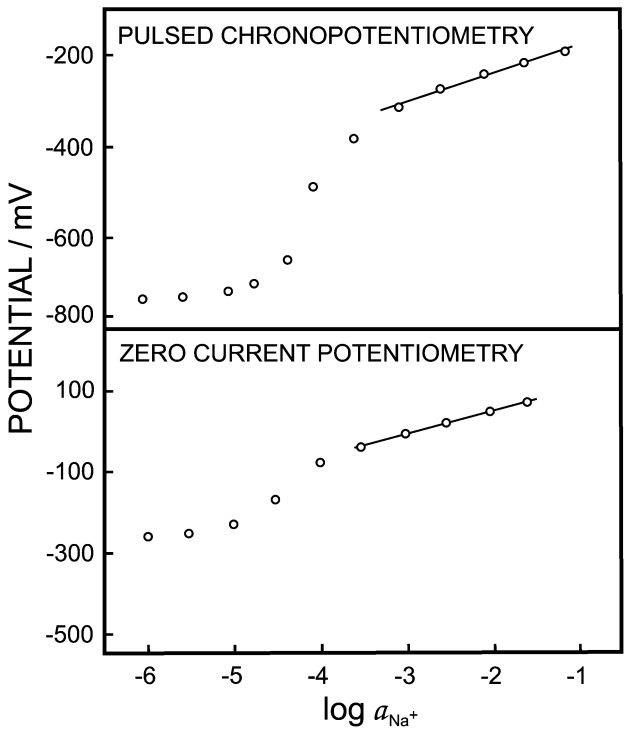

Fig. 7 Comparison between pulsed chronopotentiometric and potentiometric responses for sodium in a 10 mM of $MgCl_2$ background electrolyte. (a) Pulsed chronopotentiometric response. Membrane composition: sodium ionophore (10 mM), ETH 500 (90 mM), PVC–oNPOE (1 : 2 mass ratio). (b) Potentiometric response. Membrane composition: sodium ionophore (10 mM), KTFPB (10 mM) and PVC–oNPOE (1 : 2 ratio).[47]

protamine).[51] The determination of hydrophilic anions (chloride) in a matrix that contains lipophilic anions such as salicylate was also reported.[52] The salicylate concentration at the membrane–sample side was reduced (by depletion) during the galvanostatic pulse, allowing one to determine chloride ions without interference or long term poisoning effects.

2.5 Flash chronopotentiometry

A related approach is focused on the analysis of the shape of the potential signal during the galvanostatic pulse as a function of time (chronopotentiometric response). This approach has opened new horizons to interrogate polymeric membranes in a matter of seconds (1–5 s), providing different information than pulstrodes. The basis of this technique was widely studied by Bard and other researchers, but always with oxidation–reduction reactions on common electrodes.

If one-dimensional diffusion theory is applied to the system, a transition time (τ) can be predicted by the Sand equation, which describes the time required for analyte depletion at the membrane surface:

$$\tau \approx \pi D_{I^+}^{\alpha} \left(\frac{c_{I^+}^{*} FA}{2i} \right)^2 \quad (10)$$

This simple equation does not consider the membrane with its corresponding selectivity properties and one assumes that the current is limited by ion diffusion in the aqueous phase. The transition time is a function of the diffusion coefficient, the bulk concentration of the analyte $c_{I^+}^{*}$ and the applied current density (i/A).

Note that with most dynamic electrochemistry techniques the sensor response is a function of the concentration (diffusion theory) instead of the activity of the primary analyte (Nernst equation). As demonstrated in the literature, a combination of dynamic and static electrochemistry techniques allows one to obtain more complete and general information about the sample. Indeed, this synergy was utilized to distinguish total and free ions such as calcium[53] and protons (pH and acidity)[54] in diluted human blood and vinegar samples, respectively. The sample speciation was performed using two different membrane compositions. One was operated under controlled current (in the absence of ion-exchanger) and another interrogated by potentiometry (with ion-exchanger in the membrane). This promising approach may be valuable for monitoring dynamic biological and environmental processes.

Furthermore, localized ion-depletion was not only used for detecting small hydrophilic ions but also for polyions such as protamine/heparin and enzymes.[55,56] Meyerhoff has pioneered the detection of such polyions employing potentiometric polymeric membranes.[57] However, the spontaneous extraction of these charged molecules into the membrane phase complicate the potentiometric measurements because they give rise to continuous signal drift and irreversible responses. Subsequently, Bakker and Meyerhoff explored localized ion depletion of protamine and heparin in separate work.[56,58] Even though the results were significant, the selectivity of the membranes were not sufficient to detect these important drugs in undiluted whole human blood.

2.6 Thin layer coulometry

The groups of Sanchez-Pedreno and Osakai reported on the concept of ion-transfer voltammetry in flow systems.[59,60] Coulometric determination of very lipophilic ions was reported using this approach, although with non-optimal coulometric efficiency. For this study, the plasticized PVC membrane was only doped with a lipophilic salt.

Subsequently, Kihara *et al.* offered the first description of small hydrophilic ion determination with organic phases containing ionophores.[61–63] In the latter case, a porous Teflon tube (porosity of 1 μm) doped with an organic solvent that contains the ionophore and lipophilic salt was employed as a membrane. This elegant work suggests that the absolute detection of ionic species is feasible with this approach and Kihara must be credited to establish the concept of thin layer coulometric ion detection by ion transfer voltammetry. The relatively large quantities of required organic solvent and therefore of specialty chemicals might limit the analytical application of this approach. Later, Bakker *et al.* offered an alternative approach using ion-selective membranes, see further below.

2.7 All-solid state membrane electrodes

With a view to developing robust sensors that work under more extreme conditions such as high pressure, different positions,

absence or presence of sunlight, presence of proteins that can be adsorbed, *etc.*, solid state ion sensing membranes have recently been developed.

Even though selective membranes have exhibited attractive analytical characteristics in the operating modes described above, the introduction of solid contact ion-to-electron transducers may produce a new generation of sensors, as accomplished with potentiometric ion-selective electrodes in the past.[64,65]

Conducting polymers such as PEDOT or POT have already been explored as solid contact ion-to-electron transducers for the detection of small hydrophilic ions by ion-transfer voltammetry. This is a very interesting approach which prevents the counter-ion extraction at the inner membrane side (Fig. 8a). A few μm thin plasticized PVC membranes doped with an ionophore are placed on top of a conducting polymer film. Sample anions may be drawn from the sample to the PVC film by the oxidation of the conducting polymer, since the oxidation pulls an anion from the lipophilic electrolyte into the PVC film, hence creating a void that must be filled with sample anions. The extraction of sample cations may be accomplished by the incorporation of a lipophilic cation-exchanger into the thin PVC film. Alternatively, a different conducting polymer, poly(3,4-ethylendioxythiophene) (PEDOT), was demonstrated to be suitable for the extraction and accumulation of cationic sample species.

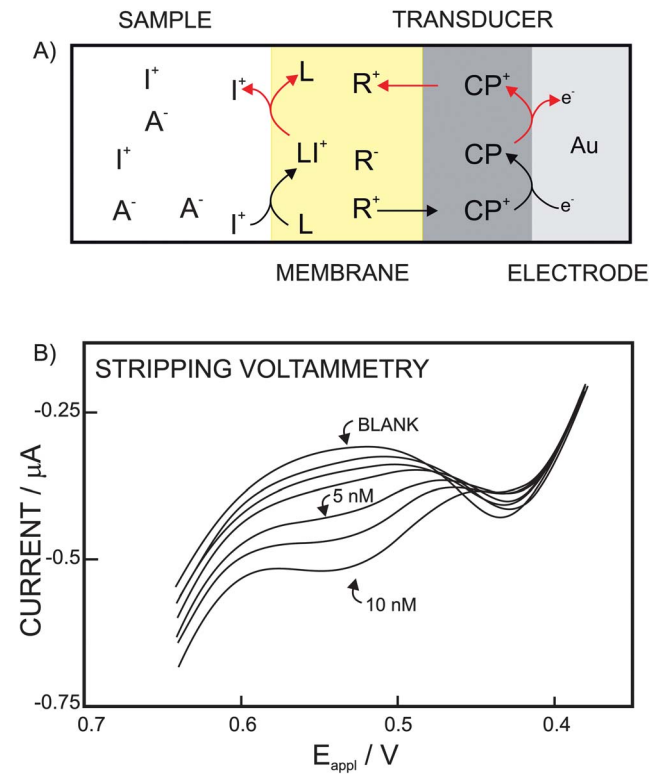

Fig. 8 Ion transfer voltammetric stripping wave for potassium ion using an all solid-state electrode.[68] (a) Illustration of the involved mechanism. Conducting polymers (CP) such as POT or PEDOT can be incorporated in the membrane and act as ion-to-electron transducer. Reduction of CP provokes a cation extraction to the membrane. (b) Ion transfer voltammetric stripping for nM level detection of potassium.

Because of the poor redox capacity of these materials, most of the literature is focused on the lower detection limits that require small currents on the order of hundreds of nA. Low detections limits on the order of nM were obtained by stripping voltammetry for potassium and perchlorate (Fig. 8b).[66–68] A higher current density might exhaustively deplete the conducting polymer at the surface of the electrode and become the undesired, current limiting step.

A different strategy, in order to overcome the mentioned limitations for conducting polymers, was reported by Langmaier *et al.*[12] Partial lipophilic ferrocene (dimethylferrocene, DMFc), which is a well-known electroactive material and has higher redox capacity than conducting polymers, was freely dissolved in the polymeric membrane. DMFc was embedded in a polymeric non-perm-selective membrane containing PVC, an apolar plasticizer (DOS) and lipophilic salts. The oxidation of DMFc creates cationic sites in the metal–membrane interface during the amperometric pulse. Therefore, anions have to be extracted from the sample into the membrane in order to compensate for the unbalanced charge. This approach was suggested for sensors capable of determining heparin (antidote of protamine) in artificial buffered samples.

A similar concept was used by Pawlak *et al.* to develop a more stable ferrocene ion-to-electron transducer for voltammetry and pulsed chronopotentiometric sensors.[69,70] Here, ferrocene was chemically attached to the PVC chain by "click chemistry" (Huisgen cycloaddition). In this manner, any leaching of the oxidized form of ferrocene (Fc^+) from the membrane to the solution is suppressed. Moreover, the concentration of ferrocene in the membrane is reduced, along with the risk of sample pollution.

3. Initially non-polarized membranes

3.1 Ion transfer electrochemistry at permselective membranes

Initially non-polarized interfaces exhibit permselective (ion-exchange) properties, in analogy to ion-selective membranes used in zero current potentiometry. Here, the analyte ion is shared between the membrane and the sample solution, which is normally accomplished by the use of an ion-exchanger (I^+R^-) in electrochemical cells of the following type:

$$RE|I^+A^-(\alpha)|I^+R^-, L(\beta)|I^+A^-(\alpha')|RE \quad (11)$$

Typically, such membranes contain also a large excess of lipophilic electrolyte to keep the membrane conductivity high (not shown). For cationic analytes as shown in eqn (11), R^- are typically tetraphenylborate derivatives. In the case of anions, lipophilic quaternary ammonium salts are normally used.

Ion exchanger compounds provide perm-selectivity to the membrane. If ion-exchange with competing ions of the same charge type is suppressed, the activity of the analyte ion in the membrane phase is determined by the concentration of the ion-exchanger (R^-). In the absence of electrochemical perturbation, the phase boundary potential at the membrane|sample solution side is a function of the activity ratio as predicted by the phase

boundary potential equation. Assuming that the membrane activity remains constant, the phase boundary potential is proportional to the activity of the analyte in the sample solution and one arrives at the established Nernst equation:

$$E_{PB} = E_I^0 + \frac{RT}{z_I F} \ln a_I^{\alpha} \quad (12)$$

If the membrane contains only an ion-exchanger, the ion-exchange selectivity is dictated by the relative lipophilicities of the competing ions. Membranes additionally doped with an ionophore may achieve an improved selectivity that is additionally dictated by the binding affinity between ionophore and analyte.

In contrast to cells containing polarizable interfaces, initially non-polarizable interfaces exhibit well defined phase boundary potential in the absence of electrochemical perturbation, allowing one to observe potentiometric information as well. Note that potentiometry is a key technique to obtain information on ion activities instead of ion concentration. This may give valuable insights into the speciation of the analyte of interest, which is important in bioanalysis and environmental analysis.

Fig. 9 illustrates the key difference between initially non-polarized and polarized membranes operated by controlled current or potential technique. When a potential is applied to an initially non-polarized membrane, the phase boundary potential is ideally still governed by eqn (1). With permselective membranes, relative activity changes in the membrane phase are much smaller than with polarizable interfaces. Moreover, the potential at the inner membrane side is defined quite naturally by an excess of I^+A^- and therefore allows for simpler experiment design and thinner membranes.

3.2 Flash chronopotentiometry

Lindner and, previously, Buck applied current perturbation on perm-selective PVC membranes.[71] It was shown that a relatively low current amplitude (hundreds of nA) can be used to compensate for the concentration gradient imposed by spontaneous ion fluxes across the membrane. In this manner, lower detection limits can be obtained by suppressing the natural fluxes that contaminate the phase boundary at the sample side.[72] Other work suggests that this technique is not very robust and cannot achieve lower detection limits than achieved by chemical optimization of the inner solution.[73]

Permselective membranes of the type shown in Fig. 9 can also be conveniently used in flash chronopotentiometry.[74] The underlying principle is identical to that explained above, where a current is applied that imposes an ion flux from the sample in direction of the membrane. A potential change at a transition time indicates the time at which the analyte ion locally depletes at the membrane surface. The use of permselective membranes allows one to use thinner membranes that exhibit faster diffusion coefficients since the membrane merely serves to shuttle the analyte ion from the sample to the inner solution. With polarizable interfaces discussed above, a counterion is instead extracted from the inner solution. A direct chemical contact of the counterion and analyte ion in the membrane must be avoided because it may result in precipitation or exudation reactions, along with the production of water droplets to accommodate this electrolyte, rendering the membranes opaque.

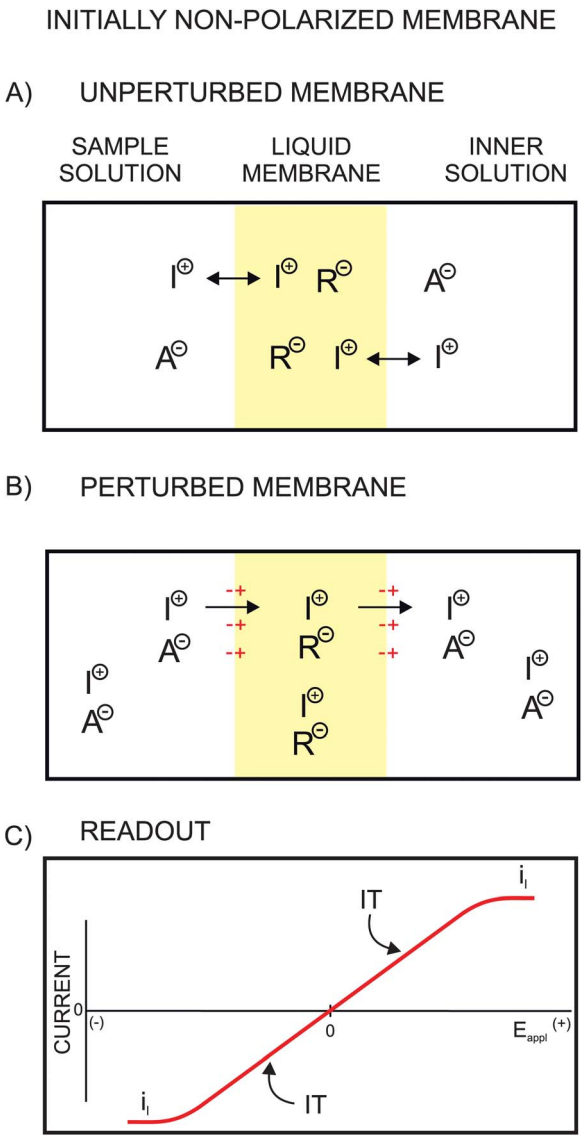

Fig. 9 Schematic illustration of the ion transfer mechanism for initially non-polarized interfaces. (a) Unperturbed membrane. The membrane contains an ion-exchanger compound (I^+R^-). Both aqueous phases contain hydrophilic components (I^+A^- for the sample and inner solution). Both boundary potentials are defined. The inner phase boundary potential is normally kept constant during the measurement. (b) Once a cathodic potential (or current) is applied to the electrochemical cell, I^+ is transported to the inner solution across the membrane. Note that the backside extraction of A^- is insignificant in this configuration. (c) Output signal for initially non-polarized interfaces (*i vs.* E_{app}) without ohmic drop compensation. The sloping line reflects the resistance of the cell (ohmic behavior). At some applied potential the interface becomes polarized and a limiting current is observed.

When the analyte is depleted the potential drastically changes to a higher potential (for cations), indicating the presence of a competing ion. The potential change is an function of the ion-exchange selectivity of the membrane. In the absence of migration, suppressed by excess background

electrolyte, the square root of the transition time is linearly proportional to the bulk concentration of the outer solution (Sand equation). This type of experiment allows one to obtain ion diffusion coefficients in the aqueous phase. The linear relationship may serve to calibrate the sensor in an analytical application.

Traditional soft polymeric liquid membranes for potassium and calcium have been used recently to develop chronopotentiometric ion sensors. A relatively narrow linear range was obtained (from 10 μM to 50 μM). Higher current amplitudes were found to limit the readout potential,[75] suggesting that the current starts to be limited by ion diffusion within the membrane rather than in the aqueous phase.

Thinner membrane materials that exhibit faster ion mobility have been subsequently explored for the purpose of developing chronopotentiometric sensors with higher detection limits. Polypropylene supported liquid membranes (of 25 μm thickness) have been introduced earlier for potentiometric detection,[76,77] although they do not give the same lower detection limits as their harder polymeric counterparts owing to faster transmembrane fluxes under zero current conditions.

The use of flash-chronopotentiometry on thin and initially non-polarizable interfaces was recently demonstrated. The first example corresponds to a single calcium perm-selective liquid membrane operated sequentially by flash chronopotentiometry and zero current potentiometry. As a result, total and free ion concentrations were quantitatively determined with a single interface. In view of developing an ion sensor for clinical analysis, total and free calcium was determined in undiluted human blood.[75] By increasing the ionophore concentration in the membrane a higher upper limit of 3 mM was also obtained. Fig. 10a shows both the chronopotentiometric and the potentiometric behavior of the optimized calcium membrane.

Local depletion is established on the basis of diffusion limitation in the aqueous layer. Mass transport induced by additional migration processes may alter the linear relationship between current, concentration and square root of transition time. This was evaluated by normalizing the square root of the transition times by multiplying them with the applied current and plotting these values as a function of the analyte concentration. Ideally, the slope now only depends on the area of the membrane and the diffusion coefficient of calcium in the aqueous phase. Fig. 10b shows both the experimental data and the behavior predicted by the Sand equation. There is a slight deviation from ideal behavior for the two highest concentrations, but the obtained diffusion coefficient of 1.23×10^{-5} cm^2 s^{-1} is in agreement with values reported in the literature. In the same work, free and complexed calcium (Ca-NTA) were distinguished. Labile complexes can be dissociated close to the membrane by the applied current if the dissociation kinetics are sufficiently rapid, as in the present case.

Chronopotentiometry at permselective membranes was successfully used for the determination of protamine (and its antidote, heparin) in heparinized and undiluted whole human blood.[78] The response mechanism is illustrated in Fig. 11a. The membrane contains a 100% molar excess of dinonylnaphthalene sulfonate, DNNS$^-$ (selective ion pair reagent for protamine) over tetradodecylammonium ion (TDDA$^+$) which is a lipophilic mono-cation with anion exchanger properties.

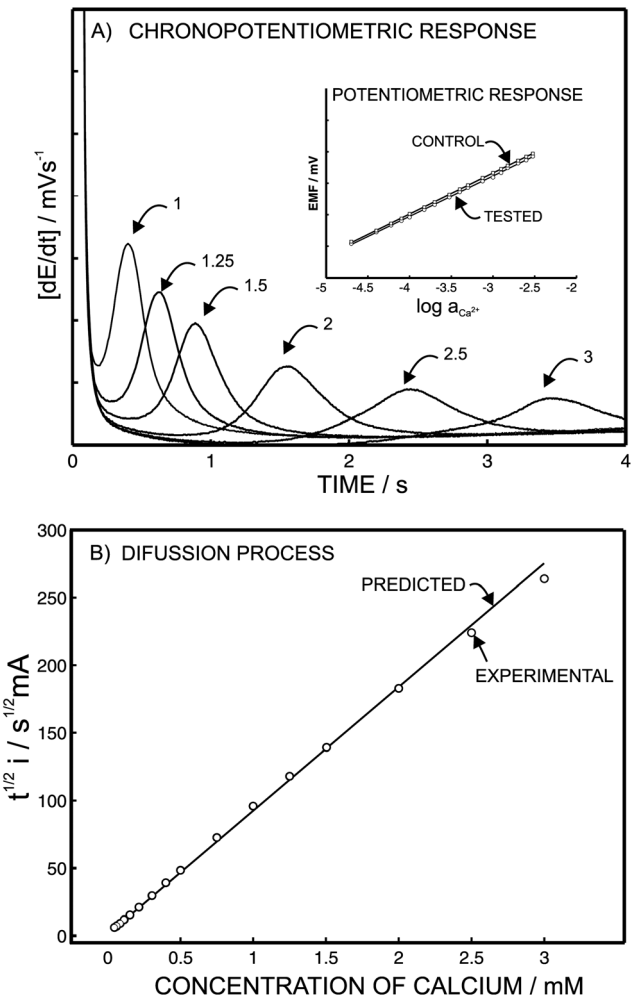

Fig. 10 Chronopotentiometric response for thin polypropylene membranes. (a) Chronopotentiometric calcium response in a wide concentration range (to 3 mM of Ca^{2+}). Inset, observed calcium calibration curves for the calcium membrane sequentially measured by potentiometry (control) and chronopotentiometry (tested). (b) Predicted and experimental normalized square root of the transition times by multiplying them with the applied current as a function of total calcium concentration. Diffusion coefficient of calcium is estimated from the slope.[75]

The main role of TDDA is to stabilize stoichiometrically the required amount of DNNS$^-$ by ion-pair interactions within the membrane in the unperturbed system. An applied constant current pulse imposes the transport of protamine from the sample across the membrane into the inner solution with a defined flux. This transport results in a required protamine accumulation at the sample side of the membrane, which is facilitated by the presence of the salt DNNS–TDDA in the membrane (Fig. 11b). Membranes containing only DNNS as an active ingredient did not give operational responses. After the transition time, a background cation such as sodium is co-extracted along with protamine to maintain the imposed ion flux, which results in a decreased membrane potential (Fig. 11c).

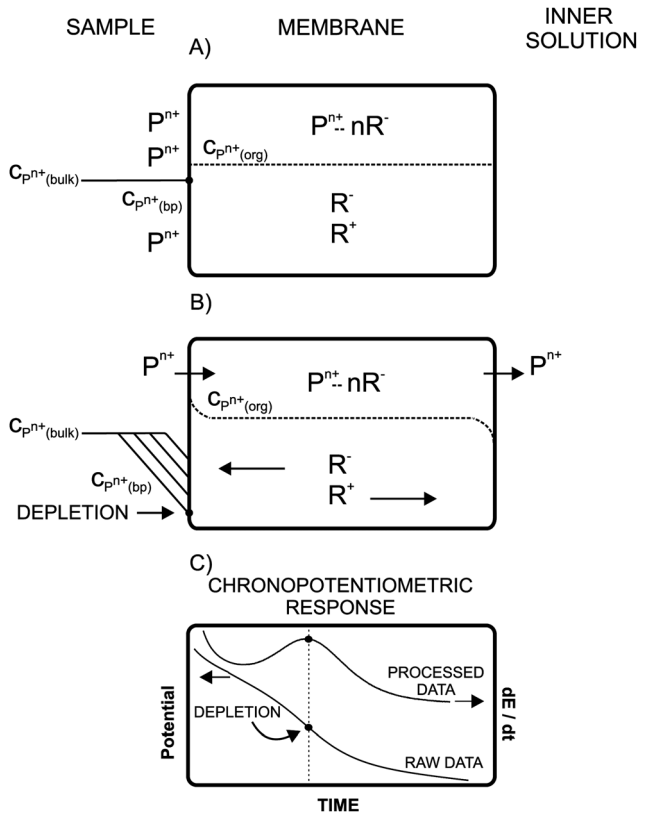

Fig. 11 Illustration of the protamine sensing mechanism. (a) The liquid membrane contains R^+ (TDDA) and protamine (P^+) bound to excess of R^- ($DNNS^-$).[78] Protamine concentration in the membrane before electrochemical perturbation is described with a dotted line. The protamine concentration in the aqueous phase ($C_P{}^{n+}$) is close to that in the phase boundary ($C_P{}^{n+}$(bp)). (b) At given applied current, a defined protamine flux across the perm-selective membrane and is sustained up to a transition time. The accumulation of protamine at the left side of the membrane during the pulse is somehow stabilized by ion-pair formation with $DNNS^-$ from the added salt DNNS–TDDA, while the liberated $TDDA^+$ migrates to the right side of the membrane to counterbalance the excess of $DNNS^-$ generated from protamine release. (c) Expected chronopotentiogram and processed chronopotentiogram of the protamine depletion.

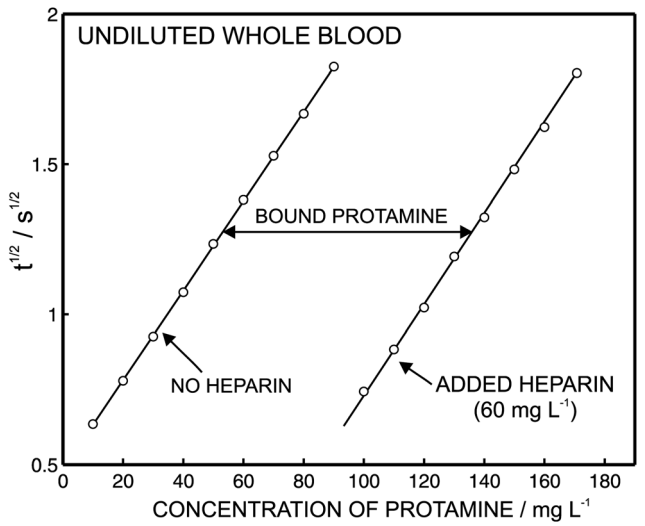

Fig. 12 Square root of transition time *vs.* protamine concentration in the absence and in presence of heparin in undiluted human blood. The amount of bound protamine during the experiment (and therefore the heparin concentration), is accurately obtained from the horizontal distance between the two linear calibration as indicated in the figure (85 mg L^{-1}).[78]

It was found that a molar ratio DNNS : TDDA of 2 : 1 gives the best selectivity for measurement of protamine in blood. The square root *vs.* concentration plot (Fig. 12) is linear, corresponding to a diffusion coefficient for protamine of 7.83×10^{-6} cm^2 s^{-1}. In a separate experiment another blood sample was spiked with 60 mg L^{-1} (final concentration) of heparin. Protamine additions gave visible transition times at above 85–90 mg L^{-1} added protamine, consistent with the known binding stoichiometry between heparin and protamine. The corresponding dose–response shown in Fig. 12 is linear and exhibit nearly the same slope, however an offset is observed that corresponds to the amount of protamine bound to heparin in the blood sample. This approach appears to be the most promising heparin detection methodology reported thus far and hospital correlation experiments are in progress (see ref. 79).

A current pulse of opposite sign may also drive ions from the membrane into the sample. This was successfully used to precisely deliver calcium to a bulk sample in order to effect coulometric EDTA titrations.[80] However, such outward fluxes can also be used in localized titrations. In a recent example, total acidity (cathodic current pulse), total alkalinity (anodic current pulse) and pH (by zero current potentiometry) were recently determined using a single liquid hydrogen ion-selective membrane.[81] Alkalinity is determined by imposing a defined flux of hydrogen ions from the membrane to the sample with an anodic current. The transition time at which the base species at the membrane–sample interface depletes, again due to diffusion limitation, is related to sample alkalinity. Acidity determination was accomplished in a similar manner to that of calcium depletion when a cathodic current is applied. This approach may develop into an attractive analytical tool for *in situ* determinations of aquatic systems such as lakes, rivers and oceans.

3.3 Coulometry and thin layer coulometry

Our group has recently suggested the use of thin layer perm-selective membranes as coulometric sensors.[82,83] This approach builds on previous work by Kihara and others using polarizable interfaces (see above). This concept aims to develop ion-selective sensors that do not require recalibration in the field or away from controlled laboratory conditions.

In order to maximize the exposed membrane area towards the inner and sample solution, tubular polypropylene membranes doped with the respective components (ionophore and ion-exchanger) were selected (Fig. 13). A silver/silver chloride wire was inserted in the propylene tube as an internal reference electrode (the sample must contain chloride in the background to guarantee a stable potential at this element). The gap between the wire and the membrane defines the volume of the thin layer. The electrochemical cell is otherwise as shown in eqn (11).

Once a sufficiently large potential is applied to both interfaces, the ion is transported from the thin sample layer to the outer solution. Considering that the current is only limited by ion transport on the sample side, the concentration profile starts to flatten and is gradually reduced to zero. Ideally, the analyte in the thin sample layer is exhaustively depleted, allowing for an absolute measurement. Fig. 14 compares the concentration profiles in the course of a thin layer and a typical bulk sample experiment.

Exhaustive ion depletion in the thin layer sample may be accomplished with an appropriate potential applied during a specific time. The integrated decaying current serves as the readout signal. This ion transfer charge is ideally linear with analyte concentration. Moreover, if the sample volume is known and constant, the numbers of moles of the target can be calculated by applying Faraday's law:

$$\int_0^{t_{max}} i(t)\mathrm{d}t = Fc_{I^+}^{aq}V^{aq} \quad (13)$$

If the concentration of the thin layer drops to zero and under some idealized circumstances, the electrochemical measurement becomes absolute. This may alleviate the need to recalibrate the system with standard solutions. Requirements include (i) adequate selectivity (no other ions must contribute to the measured charge), (ii) charging currents must be absent or be efficiently corrected, (iii) a defined thin layer volume and temperature, (iv) an exhaustive ion transfer during the time frame of the experiment.

Finally, the membrane is sequentially operated under potentiometric and potentiostatic modes in order to properly

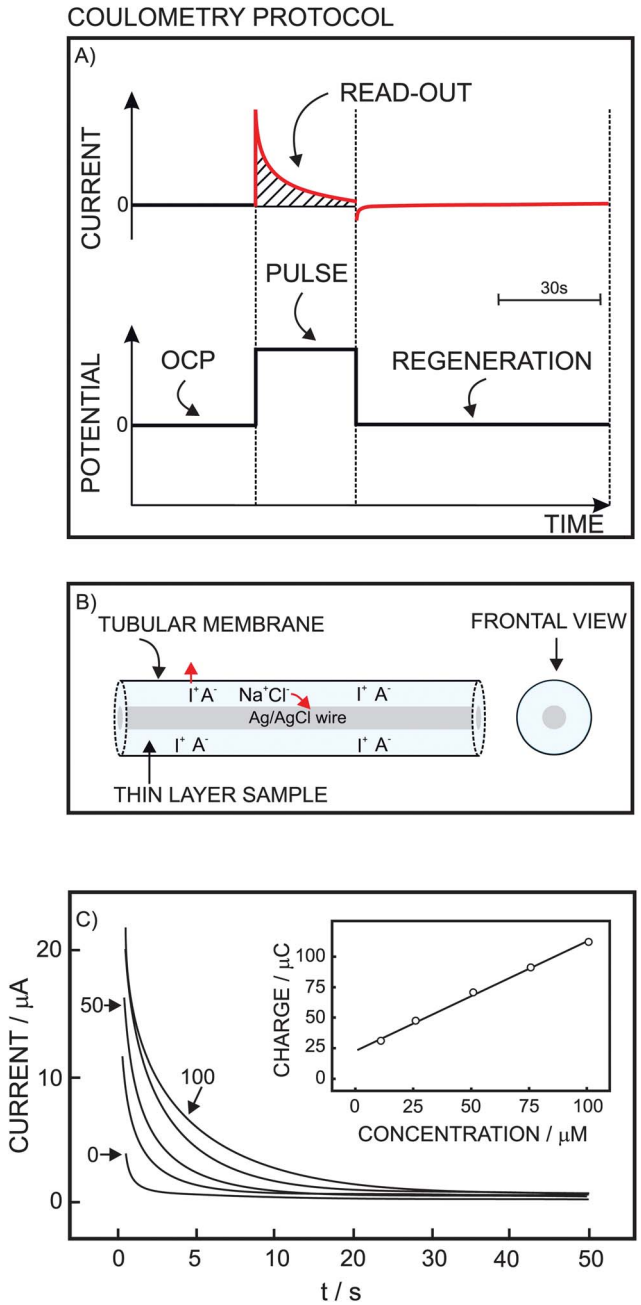

Fig. 13 An initially non-polarized polypropylene membrane interrogated by coulometry. (a) Illustration of the coulometric protocol: (i) open circuit determination; (ii) potentiostatic pulse for 60 s (output, current decay); (iii) open circuit is applied to regenerate the membrane. (b) Sketch of the thin layer sample placed between the tubular polypropylene membrane and the Ag/AgCl wire. (c) Chronoamperograms of the thin layer system. The applied potential for individual concentration is constant with respect to the open circuit potential. Inset shows the linear calibration curve between charge and concentration (observed linear range 10–100 µM of calcium). Membrane composition: 10 mM of calcium ionophore IV, 4 mM of KTFPB, 90 mM of ETH 500 and DDNPE.[82]

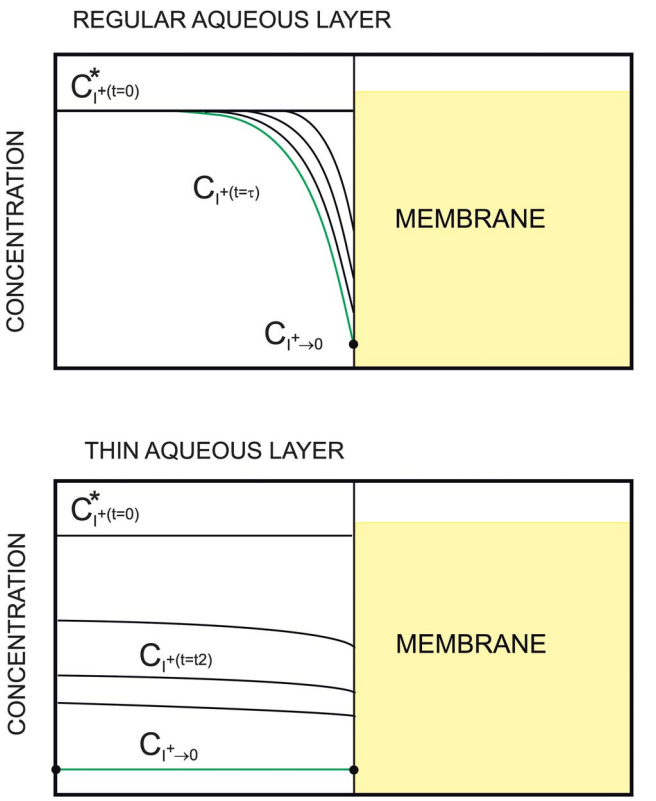

Fig. 14 Comparison between ion diffusion profiles in (a) bulk sample and (b) thin aqueous layer under controlled current or potential. In (a) localized ion-depletion is achieved at the membrane interface, but in (b) the ion target is exhaustively depleted within the thin layer.

regenerate the membrane. Some progress was made on the suppression of the background current.[84,85] This double pulse technique has been shown to drastically improve the performance of the methodology. Calibration curves show a diminished intercept, temperature influence is nearly eliminated, the operational selectivity is increased and the detection limit is lowered.[86] Other applications of nitrate detection and sodium chloride removal in seawater have been recently reported using this and related principles.[86,87]

4. Conclusions

This review outlined key principles and recent advances in the use of dynamic electrochemistry with polymeric liquid membranes. Ideally polarizable membranes are most attractive in fundamental studies of ion transfer and when the accumulation of the ion in the receiving phase is of key interest, for example in stripping ion transfer voltammetry. All solid-state membranes doped with conducting polymers have exhibited attractive low detection limit for hydrophilic ions.

On the other hand, initially non-polarized interfaces are most attractive when one aims to effect a concentration change of an ionic species in the sample phase. Conveniently, these types of membranes can be interrogated with potentiometry and sequentially with dynamic techniques such as chronopotentiometry. This can be used to obtain speciation information and total labile and free ion concentrations can be assessed under some conditions.

A number of electrochemical techniques have been reported and include controlled potential techniques such as cyclic voltammetry, normal pulse voltammetry, stripping voltammetry and thin layer coulometry as well as current controlled ones such as pulsed chronopotentiometry and flash chronopotentiometry. All of these techniques have their importance and are therefore discussed here.

Future research will most likely focus on the materials aspects of such devices in order to realize all-solid state membranes that possess the robustness, convenience and selectivity for operation in a number of important applications such as environmental monitoring and bioanalysis.

Notes and references

1 J. Koryta, *Electrochim. Acta*, 1979, **24**, 293–300.
2 D. Homolka, L. Q. Hung, A. Hofmanova, M. W. Khalil, J. Koryta, V. Marecek, Z. Samec, S. K. Sen, P. Vanysek, J. Weber, M. Brezina, M. Janda and I. Stibor, *Anal. Chem.*, 1980, **52**, 1606–1610.
3 S. Kihara, M. Suzuki, K. Maeda, K. Ogura, S. Umetani, M. Matsui and Z. Yoshida, *Anal. Chem.*, 1986, **58**, 2954–2961.
4 Z. Samec, *Chem. Rev.*, 1988, **88**, 617–632.
5 F. Reymond, D. Fermin, H. J. Lee and H. H. Girault, *Electrochim. Acta*, 2000, **45**, 2647–2662.
6 Z. Samec, *Pure Appl. Chem.*, 2004, **76**, 2147–2180.
7 B. R. Horrocks and M. V. Mirkin, *Anal. Chem.*, 1998, **70**, 4653–4660.
8 S. Amemiya, X. T. Yang and T. L. Wazenegger, *J. Am. Chem. Soc.*, 2003, **125**, 11832–11833.
9 Z. Samec, A. Trojanek, J. Langmaier and E. Samcova, *Electrochem. Commun.*, 2003, **5**, 867–870.
10 Y. Yuan and S. Amemiya, *Anal. Chem.*, 2004, **76**, 6877–6886.
11 J. D. Guo, Y. Yuan and S. Amemiya, *Anal. Chem.*, 2005, **77**, 5711–5719.
12 J. Langmaier, J. Olsak, E. Samcova, Z. Samec and A. Trojanek, *Electroanalysis*, 2006, **18**, 1329–1338.
13 G. Herzog, V. Kam, A. Berduque and D. W. M. Arrigan, *J. Agric. Food Chem.*, 2008, **56**, 4304–4310.
14 S. Amemiya, Y. Kim, R. Ishimatsu and B. Kabagambe, *Anal. Bioanal. Chem.*, 2011, **399**, 571–579.
15 C. J. Collins, C. Lyons, J. Strutwolf and D. W. M. Arrigan, *Talanta*, 2010, **80**, 1993–1998.
16 J. Strutwolf and D. W. M. Arrigan, *Anal. Bioanal. Chem.*, 2010, **398**, 1625–1631.
17 A. Berduque, R. Zazpe and D. W. M. Arrigan, *Anal. Chim. Acta*, 2008, **611**, 156–162.
18 J. Strutwolf, M. D. Scanlon and D. W. M. Arrigan, *Analyst*, 2009, **134**, 148–158.
19 M. D. Scanlon, J. Strutwolf, A. Blake, D. Iacopino, A. J. Quinn and D. W. M. Arrigan, *Anal. Chem.*, 2010, **82**, 6115–6123.
20 S. O'Sullivan and D. W. M. Arrigan, *Electrochim. Acta*, 2012, **77**, 71–76.
21 Y. Yuan, L. Wang and S. Amemiya, *Anal. Chem.*, 2004, **76**, 5570–5578.
22 P. J. Rodgers, S. Amemiya, Y. X. Wang and M. V. Mirkin, *Anal. Chem.*, 2010, **82**, 84–90.
23 V. Marecek and M. P. Colombini, *J. Electroanal. Chem.*, 1988, **241**, 133–141.
24 H. J. Lee, P. D. Beattie, B. J. Seddon, M. D. Osborne and H. H. Girault, *J. Electroanal. Chem.*, 1997, **440**, 73–82.
25 M. L. Iglehart, R. P. Buck, G. Horvai and E. Pungor, *Anal. Chem.*, 1988, **60**, 1018–1022.
26 E. Lindner, Z. Niegreisz, K. Toth, E. Pungor, T. R. Berube and R. P. Buck, *J. Electroanal. Chem.*, 1989, **259**, 67–80.
27 V. Horvath and G. Horvai, *Anal. Chim. Acta*, 1993, **273**, 145–152.
28 S. Jadhav and E. Bakker, *Anal. Chem.*, 1999, **71**, 3657–3664.
29 S. Jadhav and E. Bakker, *Anal. Chem.*, 2001, **73**, 80–90.
30 S. Jadhav, A. J. Meir and E. Bakker, *Electroanalysis*, 2000, **12**, 1251–1257.
31 M. Senda, T. Kakiuchi and T. Osakai, *Electrochim. Acta*, 1991, **36**, 253–262.
32 V. Marecek and Z. Samec, *Anal. Chim. Acta*, 1982, **141**, 65–72.
33 V. Marecek and Z. Samec, *Anal. Chim. Acta*, 1983, **151**, 265–269.
34 A. Sherburn, D. W. M. Arrigan, R. A. W. Dryfe and N. M. Boag, *Electroanalysis*, 2004, **16**, 1227–1231.
35 M. D. Scanlon, G. Herzog and D. W. M. Arrigan, *Anal. Chem.*, 2008, **80**, 5743–5749.
36 H. J. Lee, G. Lagger, C. M. Pereira, A. F. Silva and H. H. Girault, *Talanta*, 2009, **78**, 66–70.
37 A. Molina, C. Serna, J. A. Ortuno, J. Gonzalez, E. Torralba and A. Gil, *Anal. Chem.*, 2009, **81**, 4220–4225.

38 T. Ohkouchi, T. Kakutani, T. Osakai and M. Senda, *Anal. Sci.*, 1991, **7**, 371–376.
39 H. J. Lee, C. Beriet and H. H. Girault, *Anal. Sci.*, 1998, **14**, 71–77.
40 B. Huang, B. Z. Yu, P. B. Li, M. A. Jiang, Y. S. Bi and S. F. Wu, *Anal. Chim. Acta*, 1995, **312**, 329–335.
41 D. Homolka, V. Marecek, Z. Samec, K. Base and H. Wendt, *J. Electroanal. Chem.*, 1984, **163**, 159–170.
42 M. Senda, H. Katano and M. Yamada, *J. Electroanal. Chem.*, 1999, **468**, 34–41.
43 H. Katano and M. Senda, *J. Electroanal. Chem.*, 2001, **496**, 103–109.
44 C. J. Collins and D. W. M. Arrigan, *Anal. Chem.*, 2009, **81**, 2344–2349.
45 G. Herzog, A. Roger, D. Sheehan and D. W. M. Arrigan, *Anal. Chem.*, 2010, **82**, 258–264.
46 H. Katano and M. Senda, *Anal. Sci.*, 1998, **14**, 63–65.
47 A. Shvarev and E. Bakker, *Anal. Chem.*, 2003, **75**, 4541–4550.
48 S. Makarychev-Mikhailov, A. Shvarev and E. Bakker, *J. Am. Chem. Soc.*, 2004, **126**, 10548–10549.
49 E. Bakker, V. Bhakthavatsalam and K. L. Gemene, *Talanta*, 2008, **75**, 629–635.
50 A. Shvarev and E. Bakker, *Talanta*, 2004, **63**, 195–200.
51 A. Shvarev and E. Bakker, *Anal. Chem.*, 2005, **77**, 5221–5228.
52 K. L. Gemene, A. Shvarev and E. Bakker, *Anal. Chim. Acta*, 2007, **583**, 190–196.
53 K. L. Gemene and E. Bakker, *Anal. Chim. Acta*, 2009, **648**, 240–245.
54 K. L. Gemene and E. Bakker, *Anal. Chem.*, 2008, **80**, 3743–3750.
55 Y. Xu, A. Shvarev, S. Makarychev-Mikhailov and E. Bakker, *Anal. Biochem.*, 2008, **374**, 366–370.
56 K. L. Gemene and E. Bakker, *Anal. Biochem.*, 2009, **386**, 276–281.
57 J. H. Yun, M. E. Meyerhoff and V. C. Yang, *Anal. Biochem.*, 1995, **224**, 212–220.
58 K. L. Gemene and M. E. Meyerhoff, *Anal. Chem.*, 2010, **82**, 1612–1615.
59 C. Sanchez-Pedreno, J. A. Ortuno and J. Hernandez, *Anal. Chim. Acta*, 2002, **459**, 11–17.
60 S. Sawada, M. Taguma, T. Kimoto, H. Hotta and T. Osakai, *Anal. Chem.*, 2002, **74**, 1177–1181.
61 A. Yoshizumi, A. Uehara, M. Kasuno, Y. Kitatsuji, Z. Yoshida and S. Kihara, *J. Electroanal. Chem.*, 2005, **581**, 275–283.
62 M. Kasuno, K. Fujimoto, Y. Kakitani, T. Matsushita and S. Kihara, *J. Electroanal. Chem.*, 2011, **651**, 111–117.
63 S. Kihara and M. Kasuno, *Anal. Sci.*, 2011, **27**, 1–11.
64 J. Bobacka, A. Ivaska and A. Lewenstam, *Chem. Rev.*, 2008, **108**, 329–351.
65 E. Lindner and R. E. Gyurcsanyi, *J. Solid State Electrochem.*, 2009, **13**, 51–68.
66 Y. Kim and S. Amemiya, *Anal. Chem.*, 2008, **80**, 6056–6065.
67 Y. Kim, P. J. Rodgers, R. Ishimatsu and S. Amemiya, *Anal. Chem.*, 2009, **81**, 7262–7270.
68 B. Kabagambe, A. Izadyar and S. Amemiya, *Anal. Chem.*, 2012, **84**, 7979–7986.
69 M. Pawlak, E. Grygolowicz-Pawlak and E. Bakker, *Anal. Chem.*, 2010, **82**, 6887–6894.
70 M. Pawlak, E. Grygolowicz-Pawlak and E. Bakker, *Pure Appl. Chem.*, 2012, **84**, 2045–2054.
71 E. Pergel, R. E. Gyurcsanyi, K. Toth and E. Lindner, *Anal. Chem.*, 2001, **73**, 4249–4253.
72 M. A. Peshkova, T. Sokalski, K. N. Mikhelson and A. Lewenstam, *Anal. Chem.*, 2008, **80**, 9181–9187.
73 L. Hofler, I. Bedlechowicz, T. Vigassy, R. E. Gyurcsanyi, E. Bakker and E. Pretsch, *Anal. Chem.*, 2009, **81**, 3592–3599.
74 J. M. Zook, S. Bodor, R. E. Gyurcsanyi and E. Lindner, *J. Electroanal. Chem.*, 2010, **638**, 254–261.
75 M. Ghahraman Afshar, G. A. Crespo and E. Bakker, *Anal. Chem.*, 2012, **84**, 8813–8821.
76 J. Sutter, W. E. Morf, N. F. de Rooij and E. Pretsch, *J. Electroanal. Chem.*, 2004, **571**, 27–35.
77 K. Tompa, K. Birbaum, A. Malon, T. Vigassy, E. Bakker and E. Pretsch, *Anal. Chem.*, 2005, **77**, 7801–7809.
78 G. A. Crespo, M. G. Afshar and E. Bakker, *Angew. Chem., Int. Ed.*, 2012, **51**, 12575–12578.
79 E. Bakker, G. A. Crespo, M. G. Afshar, T. Saxer and K. Bendjelid, *Chimia*, 2013, **67**, 350.
80 V. Bhakthavatsalam, A. Shvarev and E. Bakker, *Analyst*, 2006, **131**, 895–900.
81 G. A. Crespo, M. Ghahraman Afshar and E. Bakker, *Anal. Chem.*, 2012, **84**, 10165–10169.
82 E. Grygolowicz-Pawlak and E. Bakker, *Anal. Chem.*, 2010, **82**, 4537–4542.
83 E. Bakker, *Anal. Chem.*, 2011, **83**, 486–493.
84 E. Grygolowicz-Pawlak and E. Bakker, *Electrochem. Commun.*, 2010, **12**, 1195–1198.
85 E. Grygolowicz-Pawlak, A. Numnuam, P. Thavarungkul, P. Kanatharana and E. Bakker, *Anal. Chem.*, 2012, **84**, 1327–1335.
86 E. Grygolowicz-Pawlak, M. Sohail, M. Pawlak, B. Neel, A. Shvarev, R. de Marco and E. Bakker, *Anal. Chem.*, 2012, **84**, 6158–6165.
87 M. Sohail, R. De Marco, K. Lamb and E. Bakker, *Anal. Chim. Acta*, 2012, **744**, 39–44.